UCSF
UC San Francisco Previously Published Works

Title
Toll-like receptor 9 signaling acts on multiple elements of the germinal center to enhance antibody responses.

Permalink
https://escholarship.org/uc/item/6wc096tf

Journal
Proceedings of the National Academy of Sciences of USA, 111(31)

Authors
Rookhuizen, Derek
Defranco, Anthony

Publication Date
2014-08-05

DOI
10.1073/pnas.1323985111

Peer reviewed

Toll-like receptor 9 signaling acts on multiple elements of the germinal center to enhance antibody responses

Derek C. Rookhuizen[a,1] and Anthony L. DeFranco[b,2]

[a]Department of Molecular and Cell Biology, Life Sciences Addition, University of California, Berkeley, CA 94720; and [b]Department of Microbiology and Immunology, University of California, San Francisco, CA 94143

Recent studies have demonstrated important roles of nucleic acid-sensing Toll-like receptors (TLRs) in promoting protective antibody responses against several viruses. To dissect how recognition of nucleic acids by TLRs enhances germinal center (GC) responses, mice selectively deleted for myeloid differentiation primary-response protein 88 (MyD88) in B cells or dendritic cells (DCs) were immunized with a haptenated protein antigen bound to a TLR9 ligand. TLR9 signaling in DCs led to greater numbers of follicular helper T (T_{FH}) cells and GC B cells, and accelerated production of broad-affinity antihapten IgG. In addition to modulating GC selection by increasing inducible costimulator (ICOS) expression on T_{FH} cells and reducing the number of follicular regulatory T cells, MyD88-dependent signaling in B cells enhanced GC output by augmenting a class switch to IgG2a, affinity maturation, and the memory antibody response. Thus, attachment of a TLR9 ligand to an oligovalent antigen acted on DCs and B cells to coordinate changes in the T-cell compartment and also promoted B cell-intrinsic effects that ultimately programmed a more potent GC response.

The ability of the innate immune system to survey infection relies on pattern recognition receptors, such as Toll-like receptors (TLRs), that signal through myeloid differentiation primary-response protein 88 (MyD88) upon recognition of pathogen-associated molecular patterns (PAMPs). Recognition of infection by TLRs shapes adaptive immunity by directing dendritic cells (DCs) to activate naive T cells (1–3), by directing T helper (T_H) 1 and T_H17 polarization of effector T cells (3, 4), and by promoting B-cell activation and terminal differentiation to antibody-secreting plasma cells (5, 6).

Following infection or vaccination, antibody responses generally proceed in two phases: an initial extrafollicular response, which rapidly generates short-lived plasmablasts that secrete low-affinity IgM and small quantities of isotype-switched antibodies (7), and a slower germinal center (GC) response, where B cells switch Ig isotype, increase affinity for antigen through somatic mutation of IgH and IgL genes, and undergo selection processes (8). Importantly, the GC builds protection from reinfection by selecting long-lived plasma cells and memory B cells from cells expressing isotype-switched, affinity-matured B-cell antigen receptors (BCRs) (9). Initially, it was proposed that TLR signaling selectively favored the extrafollicular component of serological immunity (10), but it was shown subsequently that TLR signaling in B cells could greatly augment the GC response to virus-like particles, nanoparticles, and virions (5, 11, 12). Moreover, the ability of B-cell TLRs to enhance the antibody response was recently shown to be important for host defense of mice infected with Friend virus and the chronic version of lymphocytic choriomeningitis virus (LCMV) (12–14).

Follicular helper T (T_{FH}) cells maintain the GC and govern selection for GC B cells with increased affinity for antigen (8, 15). The transcriptional repressor B-cell lymphoma-6 (Bcl-6) is essential for T_{FH} cell development and for up-regulation of the chemokine receptor CXCR5, which promotes migration into B-cell follicles. This receptor allows T_{FH} cells to access GCs,

where they provide survival and selection cues to antigen-presenting B cells through T-cell receptor (TCR) recognition of antigenic peptide–MHC II complexes, costimulatory ligand–receptor pairs, and cytokine production (8, 15, 16). Recently, it has become clear that some follicular $CXCR5^+CD4^+$T cells are thymically derived $FoxP3^+$ regulatory T cells, referred to as follicular regulatory T (T_{FR}) cells (17–22). Although their function is poorly understood at this point, T_{FR} cells appear to limit the size of the GC response (17–20).

Several studies have shown that physical linkage of a TLR7 or TLR9 ligand to a particulate antigen can substantially boost the GC response and lead to greater production of high-affinity antibody (5, 11, 12); however, the mechanisms underlying these effects are poorly understood. Moreover, previous studies were limited in their ability to compare a pathogen infection, a virus-like particle, or nanoparticle immunization with an immune response lacking PAMPs. To understand the mechanisms by which TLRs promote GC antibody responses, we created conjugates between a model protein antigen [nitrophenol-haptenated chicken gamma globulin (NPCGG)] and oligonucleotides that either contained or lacked a TLR9 ligand consensus motif, CpG. Both antigens induced robust GC responses, but the CpG-containing antigen induced more antinitrophenol (4-hydroxy-3-nitrophenyl; NP) IgG in the early response, better affinity maturation, and stronger memory antibody responses. Immunization of mice with DC- or B cell-specific deletion of MyD88 unveiled several distinct roles for TLR9 in the control of the GC reaction. In DCs, TLR9 signaling programmed the magnitude of the antibody response by increasing the number of T_{FH} cells as well as the number of antigen-specific GC B cells.

Significance

The antibody response of B lymphocytes proceeds in two phases, a rapid low-affinity response and a slower germinal center (GC) response that is responsible for high-affinity antibody, long-lived antibody-secreting cells, and high-affinity memory B cells. We have examined how immune cell recognition of foreign nucleic acid by Toll-like receptors enhances the GC response and found that it does so by multiple complementary mechanisms. Recognition of foreign nucleic acid by dendritic cells led to increased numbers of helper T cells and GC B cells. In contrast, recognition by the antigen-specific B cells promoted the selection of high-affinity B cells and their differentiation into memory B cells, both of which are central goals for vaccination.

By contrast, TLR9 signaling in B cells enhanced selection for high-affinity antibody, a class switch to IgG2a, and humoral memory responses. Changes in affinity maturation required TLR/MyD88 signaling in the responding B cells, whereas other enhancements were likely mediated through effects on the relative numbers of T_{FH} and T_{FR} cells, as well as the expression of inducible costimulator (ICOS) by T_{FH} cells. These results demonstrate that TLR9 signaling acts in multiple complementary ways to increase the magnitude and enhance the quality of GC reactions, and thereby to contribute to host defense against infection.

Results

TLR9 Signaling Enhances the GC Response. To characterize the contribution of TLR9 signaling to the GC response, we established an immunization strategy that allowed us to compare the quality of GCs reacting to antigen that either contained or lacked a TLR9 ligand. We used streptavidin to link a biotinylated form of the T cell-dependent antigen NPCGG to either a biotinylated CpG-containing oligonucleotide (CpG-NPCGG) or a control oligonucleotide lacking a CpG motif (non–CpG-NPCGG). Immunization of C57BL/6 mice with either form of the antigen induced robust expansion of total (B220^{hi}IgD^{lo}Fas$^+$) and antigen-specific (NP$^+$B220^{hi}IgD^{lo}Fas$^+$) Bcl-6$^+$ GC B cells as assessed by flow cytometry, but the numbers were about threefold greater with the CpG oligonucleotide-containing antigen (Fig. 1 A–C).

Injection of WT mice with either a non–CpG- or CpG-containing oligonucleotide in PBS without antigen confirmed that oligonucleotide alone was insufficient to stimulate NP$^+$ B cells to enter into a GC reaction (Fig. 1 B and C). Furthermore, immunization with NPCGG conjugates generated Igλ-expressing NP-binding B220$^+$IgD$^-$Fas^{hi} GC B cells, agreeing with early observations that anti-NP BCRs are frequently Igλ$^+$ (23) (Fig. 1D).

Because enumeration of total and antigen-specific GC cells exhibited the same trends, total GC B cells are depicted in the remaining experiments.

Corresponding to the expansion of NP$^+$ GC B cells, inclusion of a TLR9 ligand within the antigen boosted the total anti-NP IgG response by two- to threefold on day 14 (Fig. 2A), although both responses were of similar magnitude by day 21, when diverse affinities were measured (e.g., ELISA with NP$_{15}$-BSA) (Fig. 2 A and B). In contrast, when high-affinity anti-NP IgG was selectively measured (e.g., ELISA with NP$_1$-BSA), a substantial increase in response to the CpG-containing antigen was evident (Fig. 2 A, Lower, and B). In addition, CpG-NPCGG enhanced class switch to the highly inflammatory IgG2a^b (IgG2c) isotype, whereas immunization with non–CpG-NPCGG induced class switch to the less inflammatory IgG1 (Fig. 2C). Thus, inclusion of a TLR9 ligand in the antigen promoted the early production of IgG, whereas at later times, it enhanced affinity maturation and the class switch to IgG2a^b but had a minimal effect on overall IgG titers.

As expected from increased titers of anti-NP IgG at day 14 in mice immunized with CpG-NPCGG, these mice also demonstrated increased production of 4-hydroxy-3-iodo-5-nitrophenyl (NIP)–specific plasmablasts 14 d after immunization (Fig. 2D). To see if TLR9 stimulation also promoted the memory B-cell component of the GC reaction, we immunized mice with non–CpG-NPCGC and CpG-NPCGG and boosted both groups of mice with NPCGG in saline 7.5 wk (53 d) later. The secondary IgG response was significantly elevated in mice that were initially immunized with CpG-NPCGG, as demonstrated by the fold increase from day 53 to day 60 (day 7 postsecondary challenge) of diverse-affinity anti-NP IgG (Fig. 2E, Left). The enhanced IgG recall response was dominated by high-affinity antibody (Fig. 2 A and E, Right), which is consistent with memory B cells being
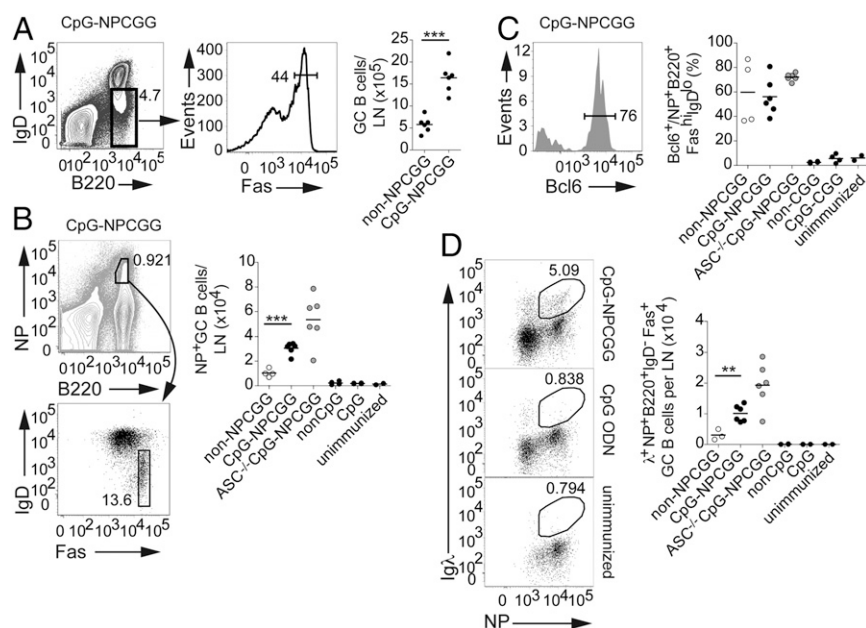
Fig. 1. Attachment of a TLR9 ligand enhances the GC response to NPCGG. (A) Flow cytometric gating logic for identification of total GC B cells (B220$^+$ IgD^{lo}Fas^{hi}) from iLNs (Left and Center) and their enumeration (Right) on day 14 after immunization, with NPCGG conjugated to non-CpG and CpG oligonucleotides (non-NPCGG and CpG-NPCGG, respectively). (B) Gating strategy for flow cytometric identification of NP-specific GC B cells (B220$^+$NP$^+$IgD^{lo}Fas^{hi}) (Left) and enumeration of total NP-specific GC B cells in the iLNs of unimmunized C57BL/6 (WT) mice or after s.c. immunization of WT and ASC$^{-/-}$ (◎) mice with either CpG- or non–CpG-containing oligonucleotides in PBS or with CpG-NPCGG or non-NPCGG (○) in PBS (Right). Each symbol represents the value obtained for a single mouse. (C, Left) Representative flow cytometric histograms from WT mice immunized with CpG-NPCGG depicting Bcl-6 expression in B220$^+$NP$^+$ IgD^{lo}Fas^{hi} cells gated as in B. (C, Right) Compiled data from duplicate experiments displaying the percentage of B220$^+$NP$^+$IgD^{lo}Fas^{hi} cells that were Bcl-6$^+$. (D) Flow cytometric analysis of Igλ$^+$NP$^+$ cells gated on B220$^+$IgD^{lo}Fas^{hi} GC B cells as in A from mice immunized as indicated (Left) and the total number of Igλ$^+$NP$^+$ B220$^+$IgD^{lo}Fas^{hi} GC B cells from the same experiments depicted in B and C (Right). **P < 0.005; ***P < 0.0001 (Student t test).
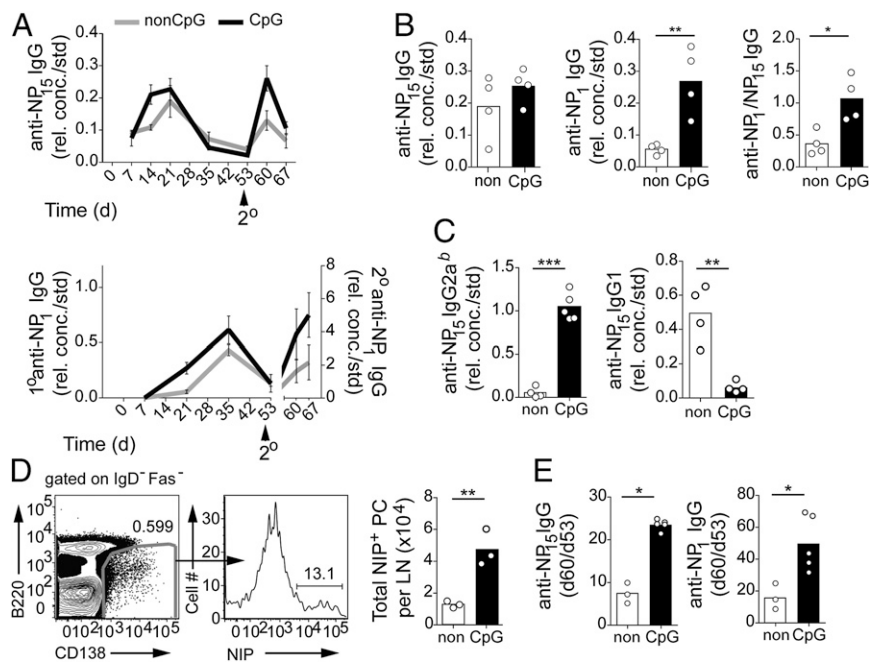
Fig. 2. TLR9 signaling boosts affinity maturation and B-cell memory. (*A*) Kinetics of primary and secondary diverse-affinity anti-NP IgG (anti-NP$_{15}$, *Upper*) and high-affinity anti-NP IgG (anti-NP$_1$, *Lower*) antibody levels following immunization of C57BL/6 WT mice with non–CpG-NPCGG (gray) or CpG-NPCGG (black) and boosted s.c. on day 53 with NPCGG in saline. (*B*) Diverse affinity (*Left*), high affinity (*Center*), and affinity maturation (ratio of anti-NP$_1$ to anti-NP$_{15}$ IgG, *Right*) of anti-NP IgG measured by ELISA at day 21 following immunization of WT mice as in *A*. (*C*) Total anti-NP IgG2a[b] and IgG1 were measured by ELISA at day 21 following immunization as in *A*. (*D*) Representative flow cytometry plots exhibiting gating scheme for enumeration of NIP-binding plasma cells (IgD$^-$Fas$^-$B220$^{int/low}$CD138$^+$NIP$^+$) (*Left* and *Center*) and data from one experiment where C57BL/6 mice were immunized with either non–CpG-NPCGG or CpG-NPCGG (*Right*). (*E*) Effect of CpG inclusion in the antigen on the secondary anti-NP IgG response. Shown is the fold increase in diverse-affinity (*Left*) and high-affinity (*Right*) anti-NP IgG titers from day 53 to day 60 (day 7 postsecondary challenge), following secondary immunization with NP-CGG in saline. Data in *B* and *C* are representative of at least six experiments, and data in *A, D,* and *E* are representation of at least two experiments. *$P < 0.05$; **$P < 0.005$; ***$P < 0.0001$ (Student *t* test). CpG, CpG-NPCGG; non, non–CpG-NPCGG; rel. conc./std., relative concentration/SD.

generated from a GC response undergoing efficient affinity maturation (9). Thus, in addition to boosting anti-NP IgG affinity and the class switch to IgG2a[b], inclusion of a TLR9 ligand linked to a protein-based antigen likely resulted in generation of more high-affinity memory B cells.

TLR9 Signaling Increases the Number and Alters the Phenotype of Follicular T Cells. The GC response is highly dependent on T$_{FH}$ cells that localize to the GC and provide selection signals for GC B-cell survival, affinity maturation, and fate decisions (15, 16). To investigate whether TLR9 signaling might enhance the GC response by having an impact on the T$_{FH}$ cell compartment, we immunized WT mice with non–CpG-NPCGC or CpG-NPCGG conjugates and measured the T$_{FH}$ cell response 14 d later. TLR9 signaling significantly boosted the total number of T$_{FH}$ cells (CXCR5$^+$PD-1$^+$CD44^{hi}CD62L^{lo}FoxP3$^-$CD4$^+$) per lymph node (LN), and also increased the percentage of activated (CD44^{hi}CD62L^{lo}FoxP3$^-$) CD4$^+$ T cells that were T$_{FH}$ cells as defined by CXCR5$^+$PD-1$^+$ expression (Fig. 3 *A* and *B*). Expression of the T$_{FH}$ cell-lineage transcription factor Bcl-6 in the draining inguinal lymph nodes (iLNs) (Fig. 3*C, Left* and *Center*), as well as in the mesenteric lymph nodes (mLNs) (Fig. 3*C, Right*), confirmed the identity of these cells. To examine whether this T$_{FH}$ cell population included antigen-specific T cells, we adoptively transferred naive OT-II TCR transgenic CD4$^+$ T cells specific for ovalbumin (OVA) into Marilyn mice that express a transgenic TCR specific for the male-restricted Y antigen (24), and then immunized with OVA conjugated to either CpG- or non–CpG-containing oligonucleotides. Immunization with the CpG-OVA conjugate induced more OT-II$^+$CD4$^+$ T cells to adopt the T$_{FH}$ cell fate (Fig. 3*D* and Fig. S1), indicating TLR9

signaling increased T$_{FH}$ cell differentiation of antigen-specific T cells.

Because the particular cytokine and costimulatory signals provided by T$_{FH}$ cells contribute importantly to GC outcome (16), we investigated whether the presence of a TLR9 ligand shaped the characteristics of the T$_{FH}$ cells. CpG-NPCGG immunization produced striking effects on cell surface expression of the costimulatory family molecules ICOS and PD-1 by T$_{FH}$ cells. Surface expression of ICOS was enhanced on T$_{FH}$ cells by three- to four-fold, on average, in mice immunized with CpG-NPCGG compared with those immunized with non–CpG-NPCGG (Fig. 3*E*); furthermore, this was selective for the T$_{FH}$ cell population because effector T cells only modestly increased their expression of ICOS (Fig. 3*E*). Interestingly, ICOS ligand (ICOSL) expression on GC B cells was not altered by the presence of a TLR9 ligand attached to the antigen (Fig. S2). ICOS is required for the GC reaction (25–27), but whether changes in expression level on T$_{FH}$ cells would contribute to more robust GC responses is unknown. In contrast to increased expression of ICOS on T$_{FH}$ cells, attachment of a TLR9 ligand to NPCGG led to decreased expression of PD-1 on the majority of T$_{FH}$ cells (Fig. 3*F* and Fig. S3*A*). Because PD-1 expression is commonly used to define T$_{FH}$ cells by flow cytometry, for this analysis, we gated on CD4$^+$ T cells expressing the T$_{FH}$ cell-inducing transcription factor Bcl-6 (Fig. 3*F*). Previous work demonstrated that a population of PD-1^{lo}Bcl-6$^+$CD4$^+$ T cells promoted extrafollicular antibody responses before full maturation to GC-localized T$_{FH}$ cells (28). To exclude the possibility that the decrease in PD-1 expression was due to the presence of non-GC Bcl-6$^+$ T cells, we quantified the number of CD4$^+$ T cells localized in the GCs and follicles of CpG-NPCGC– and non–CpG-NPCGG–immunized WT mice by immunofluorescence.

Fig. 3. TLR9 ligand increases the numbers of T_{FH} cells and alters their phenotype. (*A*) Representative flow cytometry plots of CD4$^+$ T cells depicting the T_{FH} cell-gating scheme (CD62L^{lo}B220^{lo}FoxP3$^-$CD44^{hi}PD-1$^+$CXCR5$^+$). (*B*) Frequencies and numbers of T_{FH} cells 14 d after immunization with CpG-containing or non–CpG-containing NPCGG conjugates. (*Left*) Frequency of T_{FH} cells determined as shown in *A* and displayed as a percentage of activated (CD44$^+$CD62L^{lo}) CD4$^+$ T cells. (*Right*) Total number of T_{FH} cells per LN. (*C, Left*) CD62L^{lo}B220^{lo}FoxP3$^-$CD44^{hi}PD-1$^+$CXCR5$^+$ cells displayed in *A* are Bcl-6$^+$ as shown by representative flow cytometry histograms comparing Bcl-6 expression in T_{FH}, effector T (T_{EFF}), and naive CD4$^+$ T cells from draining iLNs. (*C, Right*) Bcl-6 staining in the T_{FH}, T_{EFF}, and naive CD4$^+$ T cells from mLNs of the same mouse as a positive control for identification of T_{FH} cells. %Max, relative number of cells per channel. (*D*) Number of OT-II$^+$ T_{FH} cells as a percentage of total OT-II$^+$CD4$^+$ T cells in recipient transgenic Marilyn TCR mice 12 d after immunization with OVA conjugated to either CpG- or non–CpG-containing oligonucleotides. unimmu, unimmunized. (*E* and *F*) Effect of TLR9 ligand on T_{FH} cell expression of ICOS and PD-1. (*E, Left*) Flow cytometry histogram of ICOS expression on nonfollicular CD4$^+$ T cells (B220^{lo}CXCR5$^-$, filled gray) and T_{FH} cells from LNs of non–CpG-NPCGG– (open gray) and CpG-NPCGG–immunized mice (open black). (*E, Right*) ICOS expression represented as median fluorescence intensity (MFI) of T_{FH} cells and effector CD4$^+$ T (T_{EFF}) cells (CD62L^{lo}B220^{lo}CD44^{hi}CXCR5$^-$FoxP3$^-$). (*F, Left*) Representative flow cytometry plots depicting Bcl-6 and CXCR5 expression on CD4$^+$FoxP3$^-$CD44^{hi}CD62L^{lo} T cells. (*F, Center*) Histograms of PD-1 expression on naive T cells (filled histogram) and T_{FH} cells from either a CpG-NPCGG– or non–CpG-NPCGG–immunized mouse (color-coded as in *E*). (*F, Right*) PD-1 expression represented as MFI of T_{FH} cells. (*G, Left*) Frozen iLN sections from CpG-NPCGG– or non–CpG-NPCGG–immunized WT mice were labeled with anti-GL7-FITC (green) and anti–IgD-Alexa647 (red) to delimit GCs and follicles, respectively. Accumulation of T_{FH} cells within these regions was revealed by anti–CD4-V450 (*G, Left*, blue) and quantified using ImageJ freeware (National Institutes of Health) (*G, Right*). ns, not significant. Open circles (○) in *B*, *F*, and *G* indicate non–CpG-NPCGG, and filled circles (●) indicate CpG-NPCGG. Open circles (○) in *D* and *E* indicate T_{EFF} cells, and closed circles (●) indicate T_{FH} cells. In *B* and *D–F*, an unpaired Student *t* test was performed, and statistical significance is indicated as in Fig. 1. In *G*, a two-way ANOVA and Bonferroni's post hoc analysis for comparison of individual groups were performed. *$P < 0.05$; **$P < 0.001$.

We observed a significant increase in the accumulation of CD4$^+$ T cells in GCs when CpG-containing oligonucleotides were attached to antigen (Fig. 3*G*), indicating that the T_{FH} cells with reduced PD-1 expression were localized to the GC.

To characterize the quality of follicular helper CD4$^+$ T cells induced by the two different immunizations further, we amplified

mRNAs encoding hallmark helper T-cell cytokines from sorted T_{FH} cells and measured their levels by quantitative RT-PCR. IL-21, which affects T_{FH} cell maintenance, affinity maturation, and GC B-cell fate decisions (29, 30), exhibited a modest but significant increase in its mRNA in T_{FH} cells from mice immunized with CpG-NPCGG (Fig. S3*B*), possibly reflecting increased

ICOS signaling (31). Interestingly, inclusion of a TLR9 ligand in the antigen resulted in substantially decreased IL-4 mRNA and increased IFN-γ mRNA (Fig. S3B), which is consistent with the observed increase in isotype switching to IgG2a^b (32, 33). Thus, differential modulation of cytokine and costimulatory pathways of T$_{FH}$ cells likely established distinct selection pressures in the GC reactions occurring in the presence or absence of a TLR9 ligand. These data indicate that TLR9 stimulation led to increased numbers of T$_{FH}$ cells within the GC and also affected the T$_{FH}$ cells in qualitative ways that are consistent with the observed effects on affinity maturation and class switching.

TLR9 Signaling in DCs and B Cells Regulates the Magnitude and Quality of the GC Reaction, Respectively. Next, we wanted to determine whether modulation of T$_{FH}$ cells and GC quality by attachment of a TLR9 ligand to NPCGG was due to TLR9 signaling in DCs and/or B cells. To investigate these possibilities, we used mice that are defective in the key TLR signaling adaptor MyD88 selectively in either DCs or B cells. CD11c-Cre Myd88$^{fl/fl}$ mice delete the Myd88 gene in ~98% of conventional DCs and in about 80% of plasmacytoid DCs (referred to as DC$^{-/-}$), whereas Mb1-Cre Myd88$^{fl/fl}$ mice delete Myd88 in 98% of B cells (referred to as B$^{-/-}$) (5). As seen previously, immunization of WT mice with CpG-NPCGG induced a two- to threefold greater accumulation of total B220$^+$IgD$^-$Fas^{hi} GC B cells, compared with mice immunized with non–CpG-NPCGG. Ablation of TLR9 signaling selectively in either DCs or B cells blocked this increase (Fig. 4A). Similarly, deletion of Myd88 in DCs resulted in decreased titers of diverse-affinity anti-NP IgG (Fig. 4B) and fewer NIP-binding B220^{lo}CD138$^+$ plasma cells on day 14 (Fig. 4C). In contrast, deletion of Myd88 in B cells did not decrease the titer of diverse-affinity anti-NP IgG (Fig. 4B). Immunization of C57BL/6 and Mb1-Cre$^+$ mice with CpG-NPCGG confirmed that reduced GC B-cell formation and affinity maturation in B$^{-/-}$ mice was due to deletion of Myd88, rather than Cre-mediated toxicity (Fig. S4).

Next, we examined anti-NP IgG affinity maturation as the ratio of the amount of high-affinity anti-NP IgG to that of diverse-affinity anti-NP IgG 14 d after immunization. In WT mice, inclusion of CpG-containing oligonucleotides in the antigen boosted affinity maturation, increasing the anti-NP$_1$/NP$_{15}$ IgG ratio approximately four- to fivefold (Figs. 2 and 4B). Despite reduced GC B-cell numbers and decreased production of diverse-affinity anti-NP IgG in Myd88-DC$^{-/-}$ mice, the relative degree of affinity maturation remained intact (Fig. 4B). In contrast, mice lacking MyD88 only in B cells, which also exhibited reduced GC formation, demonstrated normal numbers of antibody-secreting plasma cells but impaired affinity maturation and a poor class switch to IgG2a^b (Fig. 4 B–D). These mice also had a reduced secondary anti-NP IgG response compared with WT mice (Fig. 4E). In contrast, MyD88 signaling in DCs only minimally affected the frequency of the class switch to IgG2a^b (both total IgG and IgG2a^b titers were reduced similarly by deletion of Myd88 in DCs) and was not required for the amplified anti-NP IgG recall following secondary immunization (Fig. 4).

The roles of MyD88 signaling in enhancing the GC response revealed by use of cell type-specific deletion of Myd88 likely reflected the effect of TLR9 signaling in DCs and B cells rather than effects of IL-1 family cytokines, whose receptors also signal via MyD88. For example, the enhanced IgG response to CpG-NPCGG compared with non–CpG-NPCGG was not attenuated by deletion of the gene encoding ASC (Fig. 1), an adaptor molecule required for assembly of most forms of the inflammasome (34), and hence required for most production of IL-1β and IL-18.

Thus, these experiments revealed that MyD88, and probably TLR9, signaling in DCs and B cells had distinct contributions to different GC outputs, including antibody quantity and quality, as
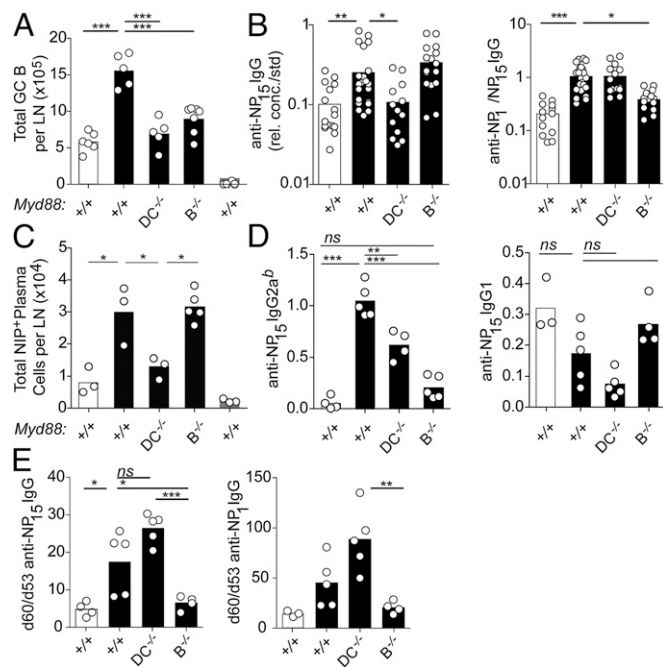
Fig. 4. TLR9 signaling in DCs and B cells controls the magnitude and quality of the GC response, respectively. (A) WT, CD11c-cre/MyD88$^{fl/fl}$ (DC$^{-/-}$), and Mb1-cre/MyD88$^{fl/fl}$ (B$^{-/-}$) mice were immunized with non–CpG-NPCGG (white bars) or CpG-NPCGG (dark bars), and the total number of GC B cells per LN was determined 14 d after immunization as described in Fig. 1. Numbers of GC B cells from iLNs of unimmunized mice are also shown (gray bar). (B, Left) Relative serum concentrations of diverse-affinity anti-NP IgG from mice with cell type-specific deletion of MyD88 were determined by ELISA 14 d after immunization with non–CpG-NPCGG (white bars) or CpG-NPCGG (black bars). (B, Right) Ratio of high-affinity anti-NP IgG to diverse-affinity anti-NP IgG as in Fig. 2B. (C) Generation of IgD$^-$Fas$^-$B220$^{int/low}$CD138$^+$NIP$^+$ plasma cells was quantified as in Fig. 2. (D) Levels of class-switched IgG2a^b (IgG2c, Left) and IgG1 (Right) anti-NP antibodies present in the serum of DC$^{-/-}$ and B$^{-/-}$ mice 14 d after immunization with CpG-NPCGG. (E) Cell type-specific requirements for TLR9 signaling to enhance the secondary anti-NP IgG response were assessed by measuring the fold increase in diverse-affinity (Left) and high-affinity (Right) IgG anti-NP antibody 7 d following secondary immunization with NPCGG in saline 53 d after the primary immunization. Statistical significance between different genotypes of mice was measured by one-way ANOVA and Bonferroni's post hoc analysis for comparison of individual groups immunized with CpG-NPCGG (A–E), and for comparison between WT ($^{+/+}$) mice immunized with non–CpG-NPCGG and CpG-NPCGG, a Student t test was performed. *P < 0.05; **P < 0.005; ***P < 0.0001. In E, statistical comparison of high-affinity titers revealed a significant difference between DC$^{-/-}$ and B$^{-/-}$ mice, but not between other groups in this particular experiment. A, B, and E represent one of four replicate experiments, C represents one of three replicate experiments, and D represents one of two replicate experiments.

well as B-cell fate decisions. Although MyD88-dependent signaling in both cell types determined GC magnitude, in DCs it boosted plasma cell development and production of diverse-affinity anti-NP IgG. In contrast, in B cells, it promoted more qualitative aspects of the GC response, such as affinity maturation, the class switch to IgG2a^b, and the secondary response, but it did not contribute to plasma cell numbers or diverse-affinity anti-NP IgG titers (Fig. 4).

TLR9-Stimulated DCs and B Cells Differentially Regulate T$_{FH}$ and FoxP3$^+$ T$_{FR}$ Cell Numbers. T$_{FH}$ cell development and maintenance is thought to be a multistage, multifactorial process accomplished by cognate interactions with DCs and B cells (15). We therefore hypothesized that TLR9 signaling in DCs and B

cells might separately control distinct aspects of the GC reaction by uniquely contributing to T_{FH} cell development and maintenance, respectively. To investigate this possibility, we examined how TLR9/MyD88 signaling in DCs and B cells affected the expansion and phenotypic properties of T_{FH} cells. MyD88 deletion in DCs compromised the burst in T_{FH} cell expansion in response to CpG-NPCGG (Fig. 5A) and reduced the number of activated $CD4^+$ T cells in the draining LN (Fig. S5), thereby leaving unaltered the frequency of T_{FH} cells relative to the number of activated T cells (Fig. 5B). These data are consistent with reduced expansion of GC B cells in these mice because multiple observations suggest that T_{FH} cell development is a limiting factor for the generation and expansion of GC B cells (35–37). In contrast, MyD88 deletion in B cells resulted in little or no reduction in total T_{FH} cell numbers following CpG-NPCGG immunization (Fig. 5A), with a more noticeable downward trend in their frequency relative to the pool of activated $CD4^+$ T cells (Fig. 5B). Thus, TLR9/MyD88 signaling in DCs boosted GC magnitude, at least in part by promoting antigen-specific activation and proliferation of CD4 T cells, a fraction of which commit to the T_{FH} cell fate.

We also examined the requirements for MyD88 in DCs and B cells for the changes in ICOS and PD-1 expression on the surface of T_{FH} cells in response to immunization with CpG-NPCGG. Although increased levels of ICOS on T_{FH} cells were partially abrogated by deletion of *Myd88* in either DCs or B cells (Fig. 5C), the effect of TLR9 signaling on T_{FH} cell expression of PD-1

was primarily due to TLR9/MyD88 signaling in DCs (Fig. 5D). Collectively, these data indicate that TLR9/MyD88 signaling in DCs and B cells had an impact on the GC reaction, at least in part by distinct effects on the T_{FH} cell compartment.

Because TLR9/MyD88 signaling in B cells had an impact on GC selection and production of high-affinity IgG but did not alter the number of T_{FH} cells, we wondered whether it could alter the recently characterized $FoxP3^+CXCR5^+$ T_{FR} cells (19, 20). Although the function of T_{FR} cells is not fully understood, it may include negative regulation of both T_{FH} cells and B cells during a GC response (17–20, 22). T_{FR} cells were identified as $CD4^+CD44^+CD62L^-PD-1^+CXCR5^+FoxP3^+$ (Fig. 5E). Five days after immunization of WT and MyD88 conditional KO mice with non–CpG-NPCGC and CpG-NPCGG, the T_{FR} cell frequency was similar among all groups (Fig. 5F). However, by day 14, the T_{FR} cell frequency in the follicular $CD4^+$ T-cell pool was decreased by threefold in WT mice that were immunized with CpG-NPCGG conjugates compared with the non–CpG-NPCGG conjugates (Fig. 5 E and G). At day 14, total T_{FR} cell numbers per LN increased in mice immunized with CpG-containing antigen (Fig. 5H), but this expansion was balanced by an even greater increase in the number of T_{FH} cells (Fig. 5A). Interestingly, there was no effect of inclusion of a TLR9 ligand bound to the antigen on the number of regulatory T cells as a frequency of activated $CD4^+$ T cells in the nonfollicular ($CXCR5^-$) component of the $CD4^+$ T-cell response (Fig. 5I). Together, the data demonstrate that the presence of a TLR9 ligand conjugated to a protein antigen preferentially
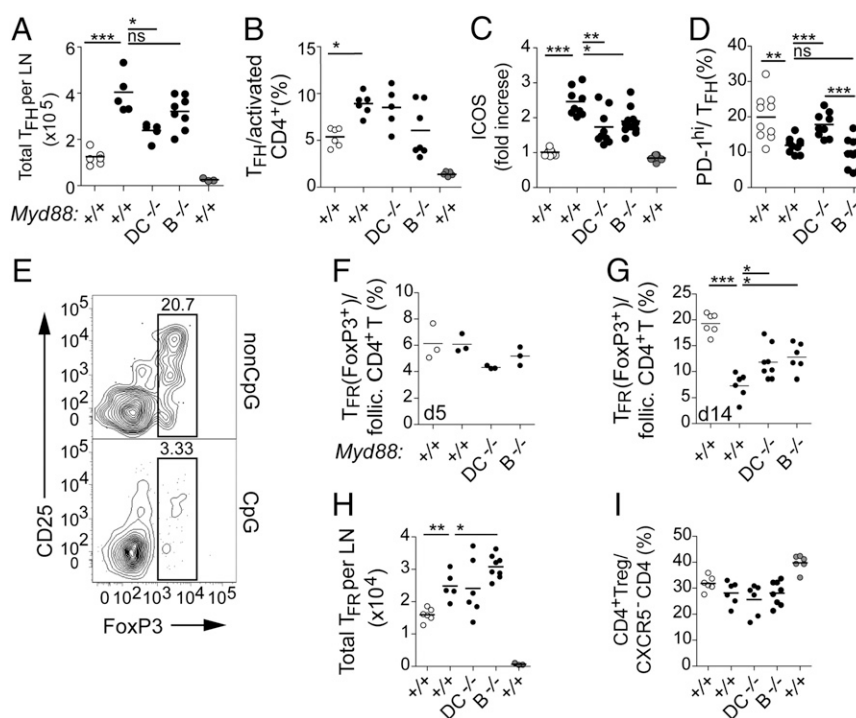
Fig. 5. TLR9 signaling in DCs and B cells determines T_{FH} cell numbers and phenotype and preferentially favors their expansion over T_{FR} cells. WT mice ($^{+/+}$) and mice deleted for *Myd88* selectively in DCs or B cells were immunized with non–CpG-NPCGG (empty circles) or CpG-NPCGG (black circles) as in Fig. 1 and analyzed by flow cytometry 14 d later. Numbers of T_{FH} cells from unimmunized mice are also shown (gray circles). (A) Total numbers of T_{FH} cells per LN. (B) Pooled data showing frequency of T_{FH} cells ($PD-1^+CXCR5^+$) from WT, $DC^{-/-}$, and $B^{-/-}$ mice as a percentage of activated $CD4^+$ T cells ($CD62L^{lo}CD44^{hi}$ $FoxP3^-$). (C) Cell surface expression of ICOS (MFI) of T_{FH} from the draining LNs, displayed as the fold increase relative to WT mice immunized with non–CpG-NPCGG. (D) Percentage of PD-1^{hi} T_{FH} cells, gated as in Fig. S2, in WT and MyD88 conditional KO mice. (E) Shown are representative flow cytometry plots of $CD4^+CD44^+$ $CD62L^{lo}PD-1^+CXCR5^+$ T_{FH} cells from draining LNs of WT mice 14 d after the indicated immunization, showing FoxP3 and CD25 expression to define T_{FR} cells. Numbers indicate the percentage of follicular $CD4^+$ T cells that are $FoxP3^+$ in individual LNs. $FoxP3^+$ T_{FR} cells as a percentage of follicular $CD4^+$ T cells at day 5 (F) or day 14 (G) postimmunization of WT littermate control, $DC^{-/-}$, and $B^{-/-}$ mice with non–CpG-NPCGG and CpG-NPCGG, gated as in E. (H) Total number of T_{FR} cells per draining LN on day 14. (I) $FoxP3^+$ regulatory T (T_{reg}) cells as a percentage of activated extrafollicular T cells ($CD4^+CD62L^{lo}CXCR5^-CD44^{hi}CXCR5^-$) on day 14. Symbols represent individual mice. Statistical analysis was performed as in Fig. 3. A, B, and F–I represent pooled data from two of two replicate experiments; in C, WT, $DC^{-/-}$, and $B^{-/-}$ data are from three replicate experiments; and in D, WT, $DC^{-/-}$, and $B^{-/-}$ data are from four replicate experiments.

modulated the composition of follicular CD4$^+$ T cells at latter stages of T$_{FR}$ cell development, when cognate interactions between follicular T cells and B cells are required for GC maintenance (38).

Consistent with the kinetics of the effect of a TLR9 ligand on the numbers of T$_{FR}$ cells in the draining LN, the absence of MyD88 signaling in DCs did not change the magnitude of the T$_{FR}$ cell compartment, whereas it did compromise the expansion of T$_{FH}$ cells (Fig. 5A). As a consequence, the fraction of T$_{FR}$ cells as a percentage of follicular CD4$^+$ T cells was increased by loss of MyD88 signaling in DCs (Fig. 5G). In contrast, when *Myd88* was selectively deleted in B cells, total T$_{FR}$ cell numbers per LN were increased (Fig. 5H) without a significant impact on T$_{FH}$ cell numbers (Fig. 5A), Thus, the frequency of T$_{FR}$ cells within the follicular CD4$^+$ T-cell pool increased (Fig. 5G). Although MyD88 signaling in B cells and DCs had different influences on the expansion of T$_{FH}$ and T$_{FR}$ cell populations, it favored T$_{FH}$ over T$_{FR}$ cell expansion in both cases. Together, these data reveal that TLR9/MyD88 signaling in DCs and B cells controlled distinct aspects of selection pressure in the GC.

Role of Cell-Intrinsic MyD88 Signaling in B Cells for the GC Response. The qualitative effects on the GC reaction of TLR9/MyD88 signaling in B cells could result from direct effects of TLR9/MyD88 signaling on the B cells receiving this stimulation, or, alternatively, these effects could result indirectly from TLR-stimulated B cells affecting the properties of antigen-specific T$_{FH}$ and T$_{FR}$ cells. To address this mechanistic question, we first generated mixed bone marrow chimeras with B cells that were WT or deficient for MyD88 and that could be distinguished by unique expression of different Ly5 allotypes. Lethally irradiated mice were reconstituted with equal portions of either *Myd88*-B$^{-/-}$ (*Mb1-cre MyD88$^{f/f}$*, Ly5.2$^+$) and WT (Ly5.1$^+$) bone marrow or WT (Ly5.2$^+$) and WT (Ly5.1$^+$) bone marrow as a control (Fig. 6A). The absence of MyD88 signaling in B cells did not affect reconstitution of mixed bone marrow chimeras (Fig. 6A, *Lower Right*); however, following immunization of these mice with CpG-NPCGG, we observed a striking disadvantage of *Myd88$^{-/-}$* B cells in GCs from draining iLNs (Fig. 6B). Interestingly, the same trend was evident in GCs from mLNs, where there is likely to be high exposure to TLR ligands from gut microbes (Fig. 6B). Thus, TLR signaling in GC B cells gave them a cell-intrinsic advantage over GC B cells not receiving TLR signaling.

To address whether the impact of TLR9 signaling on the affinity of the secreted antibody was similarly B cell-intrinsic, we adopted a second mixed bone marrow chimera approach that took advantage of different IgH allotypes to distinguish the cellular source of antigen-specific IgG. Lethally irradiated mice were reconstituted with equal portions of either *Myd88*-B$^{-/-}$ (*Mb1-cre MyD88$^{f/f}$*, IgH^b) and WT (IgH^a) bone marrow or WT (IgH^b) and WT (IgH^a) bone marrow as a control (Fig. 6C). At day 14 postimmunization, CpG-NPCGG induced an elevated level of high-affinity anti-NP IgG2a by WT B cells, whereas less high-affinity IgG2a was made by the MyD88-deficient B cells (Fig. 6D, *Center*). Comparison of the high-affinity anti-NP IgG2a^a made in the experimental and control (WT/WT) mixed bone marrow chimeric mice (Fig. 6D, *Right*) indicated that the affinity maturation of *Myd88$^{+/+}$* B cells was not adversely affected by the presence of *Myd88$^{-/-}$* B cells. *Myd88$^{-/-}$* B cells in these mixed bone marrow chimeras made as much diverse-affinity IgG2a^b anti-NP antibody as did the *Myd88$^{+/+}$* B cells (Fig. 6D, *Right*), demonstrating that they did not have a defect in the production of lower affinity anti-NP IgG or in a class switch to IgG2a. Therefore, TLR9 signaling promoted a class switch to IgG2a^b in a B cell-extrinsic fashion, potentially by affecting the follicular CD4$^+$ T-cell compartment.
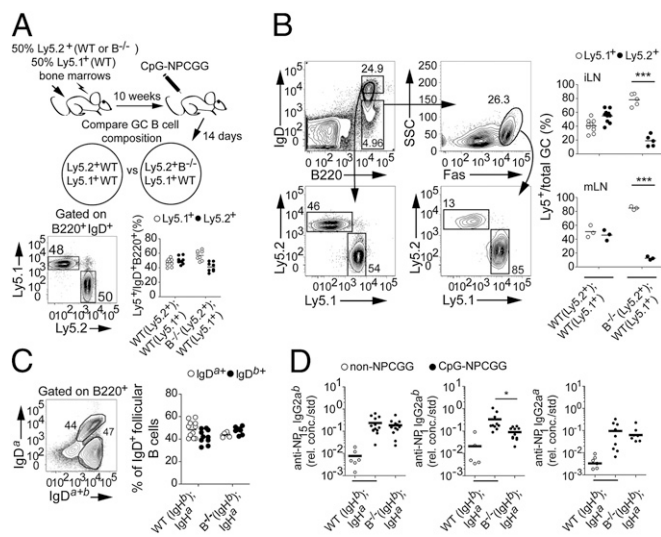
Fig. 6. B cell-intrinsic TLR9 signaling promotes affinity maturation and B-cell selection in the GC. (A) Mixed bone marrow chimeric mice were generated by reconstituting Ly5.1$^+$BoyJ mice with equal parts of either *Mb1-Cre MyD88$^{fl/fl}$*(Ly5.2$^+$) and WT(Ly5.1$^+$) bone marrow or control WT(Ly5.2$^+$) and WT(Ly5.1$^+$) bone marrow. (*Lower Left*) Reconstitution of Ly5.1$^+$ and Ly5.2$^+$ naive IgD$^+$B220$^+$ follicular B cells is shown in a representative flow cytometry plot. (*Lower Right*) Compiled percentages of cells expressing distinct Ly5 allotypes in the IgD$^+$B220$^+$ follicular B-cell population from mixed bone marrow chimeric mice. (B, *Left*) Flow cytometry analysis of Ly5.1$^+$ and Ly5.2$^+$ GC B cells (B220^{hi}IgD^{lo}Fas^{hi}) from mLNs of a representative B$^{-/-}$ (*Mb1-cre Myd88$^{fl/fl}$*) (Ly5.2$^+$):WT(Ly5.1$^+$) chimeric mouse. (B, *Right*) Number of Ly5.1$^+$ or Ly5.2$^+$ GC B cells as a percentage of total GC B cells from draining iLNs (*Upper*) or mLNs (*Lower*) 14 d after immunization with CpG-NPCGG. (C and D) Analysis of IgH allotype-marked bone marrow chimeric mice. (C) Representative flow cytometry plot showing expression of either IgD^a or IgD^b (IgD^a–IgD^{b+}) by distinct naive B-cell populations (B220$^+$) (*Left*) and compiled percentages of naive IgD^{a+} (○) and IgD^{b+} (●) B cells (*Right*). (D) Fourteen days postimmunization, the relative amounts of diverse-affinity (anti-NP$_{15}$, *Left*) and high-affinity (anti-NP$_1$, *Center*) IgG2a^b and high-affinity IgG2a^a (*Right*) were determined by ELISA as in Fig. 2. Open and closed circles represent non–CpG-NPCGG– and CpG-NPCGG–immunized mice, respectively. Statistical analysis was performed as in Fig. 4. Data are from two of two replicate experiments in which similar results were obtained.

Discussion

Although a number of studies have indicated that TLRs promote rapid production of low-affinity Ig through extrafollicular antibody responses, several recent reports have shown that TLRs can also promote GC responses (5, 11–13, 39). To analyze the mechanisms by which TLR signaling contributes to GC reactions, we turned to an oligovalent haptenated protein antigen (NP-CGG) conjugated with an oligonucleotide either containing or lacking CpG motifs. In agreement with earlier results indicating that haptenated soluble proteins are strongly immunogenic and do not require MyD88 signaling to induce vigorous antibody production (40), immunization with non–CpG-NPCGG induced a strong GC response. When the TLR9 ligand was included, however, more IgG was produced at early stages of the response, before day 21, and in addition, features associated with the quality of the GC reaction were substantially boosted. These changes were separately controlled by TLR9 signaling in DCs and B cells. TLR9/MyD88 signaling in DCs increased the magnitude of anti-NP IgG produced by promoting the expansion of T$_{FH}$ cells and GC B cells, whereas TLR9/MyD88 signaling in B cells primarily affected the quality of the GC response, resulting in better selection for high-affinity antibody, more class switching to IgG2a^b, and a stronger secondary IgG response. Taken together, these data reveal that TLR9 signaling in multiple cell

types cooperates to establish a coordinated GC reaction with characteristics previously demonstrated to be important in viral infection models, as well as in a mouse model of systemic lupus erythematosus (13, 41–44).

The enhancement of the GC reaction by the presence of a TLR9 ligand attached to the antigen was likely due, in part, to effects on the T_{FH} cell population. In our experiments, TLR9 stimulation of DCs led to an increased number of T_{FH} cells in the draining LN. Previous studies found that addition of an unlinked CpG oligonucleotide for immunization with a protein in incomplete Freund's adjuvant led to enhanced T_{FH} cell development in vivo (45) and, moreover, that this effect was dependent on TLR stimulation of monocyte-derived DCs (46). Whereas the magnitude of the GC was increased, there was no enhancement of affinity maturation (46). In that experimental system, antigen-specific B cells are unlikely to sense the presence of the CpG oligonucleotide because it was not attached to the antigen; thus, the results of those studies are largely in agreement with our conclusions regarding the effects of MyD88 signaling in DCs. In addition, we found that TLR9 signaling in DCs and/or B cells had a number of qualitative effects on the T_{FH} cell population, including up-regulation of ICOS; down-regulation of PD-1; and alterations in their cytokine profiles, namely, increased IL-21 and IFN-γ and reduced IL-4. These results add to the emerging view that full T_{FH} cell maturation occurs via two checkpoints: (i) Initial activation of naive T cells by DCs induces some of them to become T_{FH} cells, and (ii) subsequent interaction with antigen-presenting B cells induces T_{FH} cells to acquire a full GC T_{FH} cell phenotype, allowing them to enter GCs and contribute to selection (38, 47–50). Our data show that both steps are modulated by TLR9 signaling in the antigen-presenting cell to enhance the number and/or properties of T_{FH} cells.

The increased number of T_{FH} cells in the draining LNs of mice immunized with CpG-NPCGG were likely responsible for the increased numbers of GC B cells and the enhanced magnitude of the IgG anti-NP response due to TLR9/MyD88 signaling in DCs. For example, adoptive transfer of WT in vitro-differentiated T_{FH}-like cells into WT mice increased the magnitude of the GC response, indicating that the numbers of T_{FH} cells can be limiting for GC reactions (35–37).

The impact of TLR9/MyD88 signaling in both DCs and B cells on expression of the costimulatory receptors ICOS and PD-1 by T_{FH} cells likely affected their functional properties. PD-1 is an inhibitory receptor in the context of effector T-cell responses (51), and its blockade is associated with T_{FH} cell expansion (52, 53), consistent with an inhibitory role for PD-1 on T_{FH} cells as well. ICOSL/ICOS costimulatory signals at the time of DC priming are critical for T_{FH} cell development (25–27, 38, 54). Furthermore, the degree of ICOSL/ICOS engagement has been shown to determine the size of the T_{FH} cell population (55) and to promote the localization of T_{FH} cells within the GC (56). Importantly, mutation of a negative regulator of ICOS mRNA, Roquin, leads to autoimmunity that has been attributed to overly active T_{FH} cells (57, 58). Collectively, these observations suggest that elevated levels of cell-surface ICOS programmed by TLR9 signaling in DCs and B cells may have contributed to enhanced T_{FH} cell number and/or function and likely contributed to the elevated GC.

Although T_{FH} cells can be thought of as positive regulators of GCs, most data suggest a restrictive role for T_{FR} cells (17–22, 59). We found that TLR9/MyD88 signaling in both DCs and B cells affected the relative balance between T_{FH} and T_{FR} cells in the GC. When Myd88 was deleted selectively in B cells, the numbers of T_{FR} cells were increased, whereas the numbers of T_{FH} cells were unchanged. In contrast, when Myd88 was selectively deleted from DCs, there were fewer T_{FH} cells but the numbers of T_{FR} cells were largely unaffected. Thus, TLR/MyD88 signaling in both DCs and B cells regulated distinct

follicular T-cell subsets in a complementary way that increased the number of T_{FH} cells relative to the number of T_{FR} cells. The relative balance between T_{FH} and T_{FR} cells is likely to have important functional consequences, as corroborated by a recent study demonstrating that the ratio of T_{FH} to T_{FR} cells, rather than their absolute number, was more important for determining the outcome of an antibody response (59). Additionally, several studies have shown that T_{FR} cells can directly inhibit both T_{FH} cells and B cells to control separate elements of the GC (18–20).

Our findings complement emerging evidence showing that unique properties of different pathogens and immunization strategies imprint on T_{FH} cells to define their unique cytokine and costimulatory profile and, ultimately, to specify antibody responses (16, 60–62). A possible distinguishing feature among pathogens is differential expression of TLR ligands, which may stimulate DCs to influence their cytokine expression and also their ability to promote T_{FH} cell expansion.

Stimulation of TLR9 in B cells by inclusion of a CpG oligonucleotide in the NPCGG antigen enhanced the quality and, to a lesser degree, the overall magnitude of the GC reaction. Compared with the response to non–CpG-NPCGG, the anti-NP response to CpG-NPCGG included higher affinity IgG, more class switching to IgG2a, and a stronger secondary IgG response probably reflecting increased generation of anti-NP memory B cells. Surprisingly, each of these qualitative features of the GC response was lost in mice selectively deleted for Myd88 in B cells. TLR stimulation of B cells had a combination of outcomes, including qualitative and quantitative effects on the follicular CD4$^+$ T-cell population and direct effects within the responding B cells that led to better selection for high-affinity antibody production in a cell-intrinsic way. With regard to the former effects, in mice lacking MyD88 selectively in B cells, we observed a downward trend in the representation of T_{FH} cells as a fraction of activated CD4$^+$ T cells, and their expression of ICOS was also reduced (Fig. 5), suggesting that TLR9-stimulated B cells were better able to provide signals that maintain T_{FH} cell identity, promote their survival, and/or stimulate their proliferation. In line with this interpretation, previous reports showed that antigen presentation by GC B cells resulted in higher expression of CXCR5 and costimulatory molecules, such as ICOS, on T_{FH} cells (15, 38).

Although some of the effects of TLR9/MyD88 signaling in B cells appeared to be mediated by their modulation of T_{FH} cell phenotype and the relative fraction of T_{FR} cells, the more prominent effects were intrinsic to MyD88$^{+/+}$ B cells when they were combined with MyD88$^{-/-}$ B cells in mixed bone marrow chimeric mice. The use of separate alleles of the cell surface molecule Ly5 to distinguish B cells with different genotypes in response to CpG-NPCGG revealed that Myd88$^{-/-}$ B cells in the GC were underrepresented relative to Myd88$^{+/+}$ B cells (Fig. 6B). In this experimental system, any effects of TLR signaling in B cells on T_{FH} cell function would likely be reflected equally by both types of B cells, because it is known that cognate interactions between T_{FH} cells and GC B cells are short-lived relative to the time frame of the GC responses being analyzed (63–66). Thus, B cell-intrinsic TLR9 signaling improved selection of antigen-specific B cells into the GC compartment, boosted their expansion, and/or enhanced their survival. These results agree with recent studies showing that TLR7 signaling in B cells was required for full participation in the GC responses to Friend virus and LCMV (12–14). Interestingly, the same discrimination against Myd88$^{-/-}$ cells was seen in GC B cells from the mLNs of Ly5.1/Ly5.2 chimeric animals (Fig. 6B), indicating that B cell-intrinsic MyD88 signaling contributes importantly to GC responses to gut microbiota-derived antigens. This function of MyD88 could contribute to the exaggerated susceptibility to encapsulated pathogenic bacteria in individuals who are deficient for MyD88 or IRAK4 (67). Interestingly, B cell-intrinsic MyD88 signaling enhanced the amount of secreted high-affinity IgG2a^b

but did not affect the titer of diverse-affinity IgG2a[b] (Fig. 6D). Thus, B cell-intrinsic TLR9/MyD88 signaling conferred an advantage to B cells for GC selection that translated to increased production of high-affinity IgG. In contrast, the class switch to IgG2a was similar in both *Myd88*^{−/−} and *Myd88*^{+/+} B cells in mixed bone marrow chimeras, whereas it was defective if all B cells were *Myd88*^{−/−}. Therefore, we hypothesize that *Myd88*^{+/+} B cells in the GC of mixed bone marrow chimeric mice were able to promote the ability of T$_{FH}$ cells to induce B cells of either genotype to class switch to IgG2a, for example, by production of IFN-γ (32, 33, 68). Alternatively, prior studies have demonstrated that in some immunizations, the class switch to IgG2a can be a B cell-intrinsic function of TLR9 signaling (6, 69). Thus, there may be two distinct mechanisms by which TLR signaling promotes the IgG2a class switch in vivo.

Finally, we note that the experiments presented here largely agree with a recent report by Pulendran and coworkers (11), which showed that coadministration of TLR ligands and antigen adsorbed separately to nanoparticles stimulated a potent GC response characterized by augmented affinity maturation and robust B-cell memory. In our experiments, direct linkage of a haptenated protein antigen to a TLR9 ligand in oligomeric soluble complexes also induced a vigorous GC reaction. In both systems, TLR signaling in DCs and B cells was important for the enhanced IgG response. Although the responses were different in some respects, this probably reflects the distinct physical nature of nanoparticles compared with the soluble oligovalent protein–oligonucleotide conjugates used here. In any case, we have extended the previous findings by characterizing how TLR signaling in DCs and B cells differentially informs follicular CD4+ T-cell populations, composed of both T$_{FH}$ and T$_{FR}$ cells. In addition, we identified B cell-intrinsic requirements for TLR signaling that enhanced GC selection. These mechanistic insights demonstrate that TLR signaling acts in multiple complementary ways to enhance both the quantity and quality of a GC reaction, further demonstrating the importance of TLR action in the GC response during host defense. In addition, our findings may further motivate and inform efforts to incorporate TLR ligands in the design of rational vaccines that combat infectious diseases.

Experimental Procedures

Mice. Mice carrying a floxed *Myd88* allele [*Myd88*^{fl/fl}, CBy.129P2(B6)-*Myd88*[tm1Defr]/J] were generated as described previously (2, 5) and back-crossed to the C57BL/6 background for at least 10 generations. C57BL/6 backcrossed *Mb1-Cre* (70) and *CD11c-Cre* (71) mice were crossed to *Myd88*^{fl/fl} mice to generate mice deleted for *Myd88* selectively in B cells or DCs, respectively. The following mice were obtained from The Jackson Laboratory: C57BL/6 (B6), B6.Cg-*Igh*[a]*Thy1*[a]*Gpi1*[a]/J, and B6 CD45.1 (Ly5.1+BoyJ, obtained from The Jackson Laboratory or National Cancer Institute). Marilyn mice expressing the I-A[b]–restricted H-Y–specific transgenic TCR have been previously described (24) and were a gift from O. Lantz (Institut Curie, Paris, France). Male or female cohorts between 8 and 12 wk of age were age-matched within 2 wk. Mice were housed in a specific pathogen-free animal facility at the University of California, San Francisco, and all procedures involving mice were performed with Institutional Animal Care and Use Committee approval and in accord with National Institutes of Health guidelines.

Generation of CpG-NPCGG and Non–CpG-NPCGG Conjugates and Mouse Immunizations. As described in detail in *SI Experimental Procedures*, 4-hydroxy-3-nitrophenyl–haptenated chicken gamma globulin (NP$_{15–17}$CGG;

Biomol) or OVA (Sigma) was biotinylated with biotin-sulfosuccinimidyl ester (B6352; Invitrogen) and was mixed with biotin-CpG1826 (TCCATGA-CGTTCCTGACGTT) or biotin–non-CpG1826 (TCCAGGACTTCTCTCAGGTT) (Integrative DNA Technologies) containing a phosphorothioate backbone and with streptavidin to form the conjugates. Mice were injected s.c. in the hind flanks with 50 μL of conjugate containing 0.5–0.66 mg/mL NPCGG in PBS and analyzed as described. For adoptive transfers, OT-II+ T cells from female donor mice were isolated using Miltenyi Biotec's CD4+CD62L+ T-cell isolation kit, following the manufacturer's protocol, and 10⁵ naive OT-II+ T cells were adoptively transferred into Marilyn recipient mice 2 d before immunization with CpG-OVA or non–CpG-OVA conjugates.

Flow Cytometry and Cell Sorting. Lymphocytes were harvested from iLNs by passage through a 40-mm mesh filter and incubated with fluorescent anti-bodies as described in more detail in *SI Experimental Procedures*. Antigen-binding cells were detected with NP- or NIP-labeled (Biosearch Technologies) R-phycoerythrin (P801; Invitrogen) and allophycocyanin (A803; Invitrogen). All flow cytometry data were generated on an LSRII instrument (Becton Dickinson). T$_{FH}$ cells were isolated by sorting on a MoFlo cell sorter (Dako Cytomation) after enrichment for CD4+ T cells by negative selection using a Dynal Mouse CD4 Negative Isolation Kit (catalog no. 114.15D; Invitrogen).

Bone Marrow Chimeras. To generate *Mb1-cre/Myd88*^{fl/fl}:WT mixed bone marrow chimeras with different IgH allotypes, Ly5.1+BoyJ mice (The Jackson Laboratory) were lethally irradiated and reconstituted with 3 × 10⁶ bone marrow cells composed of equal portions of bone marrows from *Mb-1cre/Myd88*[fl/fl](IgH[b]) and B6.Cg-*Igh*[a]*Thy1*[a]*Gpi1*[a]/J WT (IgH[a]) or from C57BL/6 WT (IgH[b]) and B6.Cg-*Igh*[a]*Thy1*[a]*Gpi1*[a]/J WT (IgH[a]) as a control. The same protocol was used to generate *Mb1-cre/Myd88*^{fl/fl}:WT mixed bone marrow chimeras expressing different Ly5 allotypes using either *Mb-1cre/Myd88*^{fl/fl} (Ly5.2+) and BoyJ (Ly5.1+) or C57BL/6 (Ly5.2+) and BoyJ (Ly5.1+) as a control. Chimeric mice were allowed to reconstitute for 10 wk before immunization.

Immunofluorescence. Draining LNs were embedded in optimal cutting temperature compound (Sakura Finetek), frozen on dry ice and liquid N₂, and sectioned into 7-mm slices using a Leica CM3050S cryomicrotome. Fresh sections were allowed to dry overnight at room temperature before acetone dehydration and storage at −80 °C. Thawed sections were incubated in Tris-buffered saline (pH 8.5) containing 5% (wt/vol) BSA and 3% (vol/vol) normal mouse/rat serum and anti-CD16/32 Fc block for 1 h at room temperature and GCs and T$_{FH}$ cells were visualized by labeling blocked sections with anti–IgD-allophycocyanin (Biolegend), anti-CD4 Horizon V450 (BD Biosciences), and anti-GL7-FITC (BD Biosciences). All images were captured with a Zeiss LSM 780 confocal microscope using ZEN 2011 lite software.

ELISA. Ninety-six half-well, high-binding polystyrene plates (Corning 3690; Sigma-Aldrich) were coated overnight at 4 °C or for 1 h at 37 °C with NP$_{15}$-BSA (0.5 μg per well) to capture diverse-affinity anti-NP antibodies or with NP$_1$-BSA for high-affinity anti-NP IgG. Details are provided in *SI Experimental Procedures*.

Statistical Analysis. One-way ANOVA, Bonferroni's correction for multiple groups, and Student *t* tests were performed with a 95% confidence interval using GraphPad Prism (GraphPad Software, Inc.).

1. Pasare C, Medzhitov R (2004) Toll-dependent control mechanisms of CD4 T cell activation. *Immunity* 21(5):733–741.
2. Hou B, Reizis B, DeFranco AL (2008) Toll-like receptors activate innate and adaptive immunity by using dendritic cell-intrinsic and -extrinsic mechanisms. *Immunity* 29(2):272–282.
3. Spörri R, Reis e Sousa C (2005) Inflammatory mediators are insufficient for full dendritic cell activation and promote expansion of CD4+ T cell populations lacking helper function. *Nat Immunol* 6(2):163–170.
4. LeibundGut-Landmann S, et al. (2007) Syk- and CARD9-dependent coupling of innate immunity to the induction of T helper cells that produce interleukin 17. *Nat Immunol* 8(6):630–638.
5. Hou B, et al. (2011) Selective utilization of Toll-like receptor and MyD88 signaling in B cells for enhancement of the antiviral germinal center response. *Immunity* 34(3):375–384.
6. Rawlings DJ, Schwartz MA, Jackson SW, Meyer-Bahlburg A (2012) Integration of B cell responses through Toll-like receptors and antigen receptors. *Nat Rev Immunol* 12(4): 282–294.
7. MacLennan ICM, et al. (2003) Extrafollicular antibody responses. *Immunol Rev* 194: 8–18.
8. Victora GD, Nussenzweig MC (2012) Germinal centers. *Annu Rev Immunol* 30:429–457.
9. Tarlinton DM (2008) Evolution in miniature: Selection, survival and distribution of antigen reactive cells in the germinal centre. *Immunol Cell Biol* 86(2):133–138.

10. Eckl-Dorna J, Batista FD (2009) BCR-mediated uptake of antigen linked to TLR9 ligand stimulates B-cell proliferation and antigen-specific plasma cell formation. *Blood* 113(17):3969–3977.
11. Kasturi SP, et al. (2011) Programming the magnitude and persistence of antibody responses with innate immunity. *Nature* 470(7335):543–547.
12. Browne EP (2011) Toll-like receptor 7 controls the anti-retroviral germinal center response. *PLoS Pathog* 7(10):e1002293.
13. Walsh KB, et al. (2012) Toll-like receptor 7 is required for effective adaptive immune responses that prevent persistent virus infection. *Cell Host Microbe* 11(6):643–653.
14. Clingan JM, Matloubian M (2013) B Cell-intrinsic TLR7 signaling is required for optimal B cell responses during chronic viral infection. *J Immunol* 191(2):810–818.
15. Crotty S (2011) Follicular helper CD4 T cells (TFH). *Annu Rev Immunol* 29:621–663.
16. Linterman MA, Liston A, Vinuesa CG (2012) T-follicular helper cell differentiation and the co-option of this pathway by non-helper cells. *Immunol Rev* 247(1):143–159.
17. Alexander CM, et al. (2011) T regulatory cells participate in the control of germinal centre reactions. *Immunology* 133(4):452–468.
18. Wollenberg I, et al. (2011) Regulation of the germinal center reaction by Foxp3+ follicular regulatory T cells. *J Immunol* 187(9):4553–4560.
19. Linterman MA, et al. (2011) Foxp3+ follicular regulatory T cells control the germinal center response. *Nat Med* 17(8):975–982.
20. Chung Y, et al. (2011) Follicular regulatory T cells expressing Foxp3 and Bcl-6 suppress germinal center reactions. *Nat Med* 17(8):983–988.
21. Lim HW, Hillsamer P, Banham AH, Kim CH (2005) Cutting edge: Direct suppression of B cells by CD4+ CD25+ regulatory T cells. *J Immunol* 175(7):4180–4183.
22. Lim HW, Hillsamer P, Kim CH (2004) Regulatory T cells can migrate to follicles upon T cell activation and suppress GC-Th cells and GC-Th cell-driven B cell responses. *J Clin Invest* 114(11):1640–1649.
23. Jack RS, Imanishi-Kari T, Rajewsky K (1977) Idiotypic analysis of the response of C57BL/6 mice to the (4-hydroxy-3-nitrophenyl)acetyl group. *Eur J Immunol* 7(8):559–565.
24. Lantz O, Grandjean I, Matzinger P, Di Santo JP (2000) Gamma chain required for naïve CD4+ T cell survival but not for antigen proliferation. *Nat Immunol* 1(1):54–58.
25. Tafuri A, et al. (2001) ICOS is essential for effective T-helper-cell responses. *Nature* 409(6816):105–109.
26. McAdam AJ, et al. (2001) ICOS is critical for CD40-mediated antibody class switching. *Nature* 409(6816):102–105.
27. Dong C, Temann UA, Flavell RA (2001) Cutting edge: Critical role of inducible costimulator in germinal center reactions. *J Immunol* 166(6):3659–3662.
28. Lee SK, et al. (2011) B cell priming for extrafollicular antibody responses requires Bcl-6 expression by T cells. *J Exp Med* 208(7):1377–1388.
29. Zotos D, et al. (2010) IL-21 regulates germinal center B cell differentiation and proliferation through a B cell-intrinsic mechanism. *J Exp Med* 207(2):365–378.
30. Linterman MA, et al. (2010) IL-21 acts directly on B cells to regulate Bcl-6 expression and germinal center responses. *J Exp Med* 207(2):353–363.
31. Gigoux M, et al. (2009) Inducible costimulator promotes helper T-cell differentiation through phosphoinositide 3-kinase. *Proc Natl Acad Sci USA* 106(48):20371–20376.
32. Peng SL, Szabo SJ, Glimcher LH (2002) T-bet regulates IgG class switching and pathogenic autoantibody production. *Proc Natl Acad Sci USA* 99(9):5545–5550.
33. Rubtsova K, Rubtsov AV, van Dyk LF, Kappler JW, Marrack P (2013) T-box transcription factor T-bet, a key player in a unique type of B-cell activation essential for effective viral clearance. *Proc Natl Acad Sci USA* 110(34):E3216–E3224.
34. Lamkanfi M, Dixit VM (2014) Mechanisms and functions of inflammasomes. *Cell* 157(5):1013–1022.
35. Linterman MA, et al. (2009) Follicular helper T cells are required for systemic autoimmunity. *J Exp Med* 206(3):561–576.
36. Harker JA, Lewis GM, Mack L, Zuniga EI (2011) Late interleukin-6 escalates T follicular helper cell responses and controls a chronic viral infection. *Science* 334(6057):825–829.
37. Lu KT, et al. (2011) Functional and epigenetic studies reveal multistep differentiation and plasticity of in vitro-generated and in vivo-derived follicular T helper cells. *Immunity* 35(4):622–632.
38. Choi YS, et al. (2011) ICOS receptor instructs T follicular helper cell versus effector cell differentiation via induction of the transcriptional repressor Bcl6. *Immunity* 34(6):932–946.
39. Link A, et al. (2012) Innate immunity mediates follicular transport of particulate but not soluble protein antigen. *J Immunol* 188(8):3724–3733.
40. Palm NW, Medzhitov R (2009) Immunostimulatory activity of haptenated proteins. *Proc Natl Acad Sci USA* 106(12):4782–4787.
41. Johnston RJ, et al. (2009) Bcl6 and Blimp-1 are reciprocal and antagonistic regulators of T follicular helper cell differentiation. *Science* 325(5943):1006–1010.
42. Yusuf I, et al. (2010) Germinal center T follicular helper cell IL-4 production is dependent on signaling lymphocytic activation molecule receptor (CD150). *J Immunol* 185(1):190–202.
43. Lüthje K, et al. (2012) The development and fate of follicular helper T cells defined by an IL-21 reporter mouse. *Nat Immunol* 13(5):491–498.
44. Lee SK, et al. (2012) Interferon-γ excess leads to pathogenic accumulation of follicular helper T cells and germinal centers. *Immunity* 37(5):880–892.
45. Fazilleau N, McHeyzer-Williams LJ, Rosen H, McHeyzer-Williams MG (2009) The function of follicular helper T cells is regulated by the strength of T cell antigen receptor binding. *Nat Immunol* 10(4):375–384.
46. Chakarov S, Fazilleau N (2014) Monocyte-derived dendritic cells promote T follicular helper cell differentiation. *EMBO Mol Med* 6(5):590–603.
47. Goenka R, et al. (2011) Cutting edge: Dendritic cell-restricted antigen presentation initiates the follicular helper T cell program but cannot complete ultimate effector differentiation. *J Immunol* 187(3):1091–1095.
48. Kitano M, et al. (2011) Bcl6 protein expression shapes pre-germinal center B cell dynamics and follicular helper T cell heterogeneity. *Immunity* 34(6):961–972.
49. Kerfoot SM, et al. (2011) Germinal center B cell and T follicular helper cell development initiates in the interfollicular zone. *Immunity* 34(6):947–960.
50. Deenick EK, et al. (2010) Follicular helper T cell differentiation requires continuous antigen presentation that is independent of unique B cell signaling. *Immunity* 33(2):241–253.
51. Bennett F, et al. (2003) Program death-1 engagement upon TCR activation has distinct effects on costimulation and cytokine-driven proliferation: Attenuation of ICOS, IL-4, and IL-21, but not CD28, IL-7, and IL-15 responses. *J Immunol* 170(2):711–718.
52. Good-Jacobson KL, Shlomchik MJ (2010) Plasticity and heterogeneity in the generation of memory B cells and long-lived plasma cells: The influence of germinal center interactions and dynamics. *J Immunol* 185(6):3117–3125.
53. Kawamoto S, et al. (2012) The inhibitory receptor PD-1 regulates IgA selection and bacterial composition in the gut. *Science* 336(6080):485–489.
54. Akiba H, et al. (2005) The role of ICOS in the CXCR5+ follicular B helper T cell maintenance in vivo. *J Immunol* 175(4):2340–2348.
55. Ou X, Xu S, Lam KP (2012) Deficiency in TNFRSF13B (TACI) expands T-follicular helper and germinal center B cells via increased ICOS-ligand expression but impairs plasma cell survival. *Proc Natl Acad Sci USA* 109(38):15401–15406.
56. Xu H, et al. (2013) Follicular T-helper cell recruitment governed by bystander B cells and ICOS-driven motility. *Nature* 496(7446):523–527.
57. Yu D, et al. (2007) Roquin represses autoimmunity by limiting inducible T-cell costimulator messenger RNA. *Nature* 450(7167):299–303.
58. Vinuesa CG, et al. (2005) A RING-type ubiquitin ligase family member required to repress follicular helper T cells and autoimmunity. *Nature* 435(7041):452–458.
59. Sage PT, Francisco LM, Carman CV, Sharpe AH (2013) The receptor PD-1 controls follicular regulatory T cells in the lymph nodes and blood. *Nat Immunol* 14(2):152–161.
60. Fahey LM, et al. (2011) Viral persistence redirects CD4 T cell differentiation toward T follicular helper cells. *J Exp Med* 208(5):987–999.
61. King IL, Mohrs M (2009) IL-4-producing CD4+ T cells in reactive lymph nodes during helminth infection are T follicular helper cells. *J Exp Med* 206(5):1001–1007.
62. Glatman Zaretsky A, et al. (2009) T follicular helper cells differentiate from Th2 cells in response to helminth antigens. *J Exp Med* 206(5):991–999.
63. Allen CD, Okada T, Cyster JG (2007) Germinal-center organization and cellular dynamics. *Immunity* 27(2):190–202.
64. Cannons JL, et al. (2010) Optimal germinal center responses require a multistage T cell:B cell adhesion process involving integrins, SLAM-associated protein, and CD84. *Immunity* 32(2):253–265.
65. Qi H, Cannons JL, Klauschen F, Schwartzberg PL, Germain RN (2008) SAP-controlled T-B cell interactions underlie germinal centre formation. *Nature* 455(7214):764–769.
66. Victora GD, et al. (2010) Germinal center dynamics revealed by multiphoton microscopy with a photoactivatable fluorescent reporter. *Cell* 143(4):592–605.
67. Casanova JL, Abel L, Quintana-Murci L (2011) Human TLRs and IL-1Rs in host defense: Natural insights from evolutionary, epidemiological, and clinical genetics. *Annu Rev Immunol* 29:447–491.
68. Finkelman FD, et al. (1990) Lymphokine control of in vivo immunoglobulin isotype selection. *Annu Rev Immunol* 8:303–333.
69. Jegerlehner A, et al. (2007) TLR9 signaling in B cells determines class switch recombination to IgG2a. *J Immunol* 178(4):2415–2420.
70. Hobeika E, et al. (2006) Testing gene function early in the B cell lineage in mb1-cre mice. *Proc Natl Acad Sci USA* 103(37):13789–13794.
71. Caton ML, Smith-Raska MR, Reizis B (2007) Notch-RBP-J signaling controls the homeostasis of CD8- dendritic cells in the spleen. *J Exp Med* 204(7):1653–1664.